

## Multimode four-wave mixing in an unresolved sideband optomechanical system

Zongyang Li,<sup>1,2</sup> Xiang You,<sup>1,2</sup> Yongmin Li,<sup>1,2,\*</sup> Yong-Chun Liu,<sup>3,†</sup> and Kunchi Peng<sup>1,2</sup>

<sup>1</sup>State Key Laboratory of Quantum Optics and Quantum Optics Devices, Institute of Opto-Electronics, Shanxi University, Taiyuan 030006, People's Republic of China

<sup>2</sup>Collaborative Innovation Center of Extreme Optics, Shanxi University, Taiyuan 030006, People's Republic of China

<sup>3</sup>State Key Laboratory of Low-Dimensional Quantum Physics and Department of Physics, Tsinghua University and Collaborative Innovation Center of Quantum Matter, Beijing 100084, People's Republic of China



(Received 20 December 2017; published 8 March 2018)

We have studied multimode four-wave mixing (FWM) in an unresolved sideband cavity optomechanical system. The radiation pressure coupling between the cavity fields and multiple mechanical modes results in the formation of a series of tripod-type energy-level systems, which induce the multimode FWM phenomenon. The FWM mechanism enables remarkable amplification of a weak signal field accompanied by the generation of an FWM field when only a microwatt-level pump field is applied. For proper system parameters, the amplified signal and FWM fields have equal intensity with opposite phases. The gain and frequency response bandwidth of the signal field can be dynamically tuned by varying the pump intensity, optomechanical coupling strength, and additional feedback control. Under certain conditions, the frequency response bandwidth can be very narrow and reaches the level of hertz.

DOI: [10.1103/PhysRevA.97.033806](https://doi.org/10.1103/PhysRevA.97.033806)

### I. INTRODUCTION

Optomechanical systems couple photons and phonons using radiation pressure and have emerged as powerful platforms to manipulate mechanical resonators and electromagnetic fields. Particularly, optomechanically induced transparency (OMIT) and amplification (OMIA) [1–4] have been observed in various optomechanical systems in resolved sideband regimes, where the dissipation rate of the optical mode is smaller than the resonance frequency of the mechanical resonator. In this case, only the beam-splitter interaction is involved and  $\Lambda$ -type energy levels are formed, whereas the two-mode squeezing interaction is suppressed owing to the nonresonant response of the cavity.

Four-wave mixing (FWM) is a typical nonlinear optical phenomenon achieved in various media including atomic vapors [5–10], nonlinear crystals [11], and optical fibers [12,13]. FWM has found numerous applications in the fields of nonlinear optics and quantum optics. Recently, radiation-pressure-induced FWM in a cavity optomechanical system has been investigated in a resolved sideband regime. For instance, the mechanical mode splitting arising from strong optomechanical coupling [14,15], the optical response properties of an optomechanical system with additional coherent mechanical driving [16–18], and a two-mode cavity optomechanical system with two cavity modes coupled to a mechanical resonator [19] have been investigated theoretically. However, FWM has been seldom studied in the unresolved sideband regime, where the dissipation of the optical cavity is beyond the resonance frequency of the mechanical resonator.

In this paper, we have investigated in detail the multimode FWM phenomenon of an optomechanical system in an unresolved sideband regime. In our scheme, neither strong optomechanical coupling nor additional coherent mechanical driving is required. Owing to the participation of additional two-mode squeezing interaction in the unresolved sideband regime, the radiation pressure coupling between the cavity fields and multiple mechanical modes results in the formation of a series of tripod-type energy-level schemes, which induces the multimode FWM phenomenon. When only a microwatt-level pump field is applied, the FWM mechanism enables a remarkable amplification of the weak signal field. Moreover, an FWM field with almost the same intensity as the input signal is generated simultaneously. Furthermore, the gain and frequency response bandwidth of the system can be actively tuned by changing the pump intensity, optomechanical coupling strength, and additional feedback control.

### II. THEORETICAL MODEL AND ANALYSIS OF RESULTS

We consider an optomechanical system [Fig. 1(a)] consisting of a two-mode mechanical resonator with frequency  $\omega_{m,j}$  and decay rate  $\Gamma_{m,j}$  (where  $j = 1, 2$  denotes different mechanical modes of the mechanical resonator) and an optical cavity with cavity mode frequency  $\omega_c$  and dissipation rate  $\kappa$ . We assume that the optomechanical system operates in the unresolved sideband regime where  $\kappa \gg \omega_m$ . In this case, the energy-level diagram corresponding to the coupling between the cavity fields and mechanical modes can be described using two tripod-type schemes, as shown in Fig. 1(b). A strong pump field  $a_p$ , which is resonant with the cavity, couples the transition  $|n_c, m_1, m_2\rangle \leftrightarrow |n_c + 1, m_1, m_2\rangle$ ; a weak signal field with frequency  $\omega_{s,1}$ , which is blue-detuned to the pump laser with detuning  $\Delta_{s,1} = \omega_{s,1} - \omega_p = \omega_{m,1}$ , couples the

\*yongmin@sxu.edu.cn

†ycliu@tsinghua.edu.cn

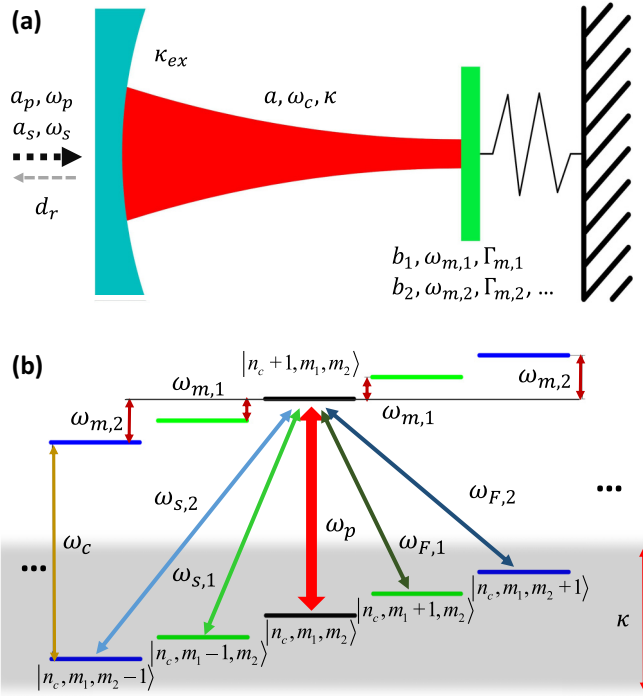


FIG. 1. (a) Model of our optomechanical system driven by a pump field and signal field. (b) Energy-level diagram of the unresolved sideband optomechanical system.  $n_c$  and  $m_j$  represent the photon number of the cavity mode and phonon number of the  $j$ th mechanical mode, respectively. The shadow with the width of  $\kappa$  represents the response bandwidth of the optical cavity. When a strong resonance pump field and weak detuned signal field are injected into the cavity, the signal field with the frequency  $\omega_{s,j} = \omega_p + \omega_{m,j}$  is amplified accompanied by an FWM field with the frequency  $\omega_{F,j} = \omega_p - \omega_{m,j}$ .

transition  $|n_c, m_1 - 1, m_2\rangle \leftrightarrow |n_c + 1, m_1, m_2\rangle$ ; and the generated FWM field with frequency  $\omega_{F,1}$  couples the transition  $|n_c, m_1 + 1, m_2\rangle \leftrightarrow |n_c + 1, m_1, m_2\rangle$ . Based on this tripod-type configuration, the input signal field can be amplified remarkably and the associated FWM field is generated simultaneously. The relevant frequencies of the FWM parametric fields follow the law of conservation of energy:  $2\omega_p \equiv \omega_{s,1} + \omega_{F,1}$ . Notably, the system behaves the same when the signal field is red-detuned to the pump laser  $\Delta_{s,1} = \omega_{s,1} - \omega_p = -\omega_{m,1}$ .

Similarly, the coupling between the cavity field and mechanical mode with frequency  $\omega_{m,2}$  can form another tripod-type configuration. More precisely, a weak signal field with the frequency  $\omega_{s,2}$  with blue-detuning  $\Delta_{s,2} = \omega_{s,2} - \omega_p = \omega_{m,2}$  couples the transition  $|n_c, m_1, m_2 - 1\rangle \leftrightarrow |n_c + 1, m_1, m_2\rangle$ , and the FWM field with the frequency  $\omega_{F,2}$  couples the transition  $|n_c + 1, m_1, m_2\rangle \leftrightarrow |n_c, m_1, m_2 + 1\rangle$ . Notably, our system intrinsically supports multiple independent FWM processes simultaneously when only one pump field is applied, if a number of mechanical modes in the optomechanical system are exploited. This is because the cavity linewidth covers multiple energy levels, which further opens up related transition pathways in the unresolved sideband regime.

In our scheme, we assume the linewidth of the mechanical susceptibility is far less than the frequency difference of adjacent mechanical modes, thus direct coupling between

different mechanical modes can be neglected. On the other hand, the intense pump laser field drives the optomechanical system to a steady state, the existence of the signal fields which are much weaker than the pump field does not change the steady state of the system, and the signal fields are treated as the perturbations of the steady state. Therefore, the presence of another weak signal field and the resulting FWM process has negligible effects on the already existing FWM process, and vice versa. Thus multimode FWM can be directly decomposed into coexisting individual single-mode FWM processes.

### A. Hamiltonian and Langevin equations

Herein for simplicity, we consider only one mechanical mode with resonance frequency  $\omega_m$  for the optomechanical interaction, thus the Hamiltonian of the unresolved sideband optomechanical system is of the form

$$\begin{aligned} H &= H_{\text{free}} + H_{\text{int}} + H_{\text{drive}}, \\ H_{\text{free}} &= \omega_c a^\dagger a + \omega_m b^\dagger b, \\ H_{\text{int}} &= g_0 a^\dagger a (b^\dagger + b), \\ H_{\text{drive}} &= i\sqrt{\kappa_{\text{ex}}}(\alpha_p e^{-i\omega_p t} a^\dagger + \alpha_s e^{-i\omega_s t} a^\dagger) + \text{H.c.}, \end{aligned} \quad (1)$$

where  $H_{\text{free}}$ ,  $H_{\text{int}}$ , and  $H_{\text{drive}}$  denote the free Hamiltonian, optomechanical interaction part of the Hamiltonian, and optical driving of the system, respectively;  $a$  denotes the annihilation operator of the optical cavity mode with angular frequency  $\omega_c$ ;  $b$  denotes the annihilation operator of the mechanical mode with angular frequency  $\omega_m$ . The displacement operator  $x$  is related to the mechanical mode operators as  $x = x_{\text{ZPF}}(b^\dagger + b)$ , where  $x_{\text{ZPF}} = \sqrt{\hbar/2m_{\text{eff}}\omega_m}$  is the zero-point fluctuation and  $m_{\text{eff}}$  is the effective mass of the mechanical mode.  $g_0 = x_{\text{ZPF}}[\partial\omega_c(x)/\partial x]$  denotes the single-photon optomechanical coupling strength.  $\omega_p$  and  $\omega_s$  denote the laser angular frequencies of the pump and signal fields with driving strengths  $\alpha_p = \sqrt{P_p/\hbar\omega_p}e^{-i\phi_p}$  and  $\alpha_s = \sqrt{P_s/\hbar\omega_s}e^{-i\phi_s}$ , respectively, where  $P_p$ ,  $P_s$  and  $\phi_p$ ,  $\phi_s$  denote the input powers and initial phases of the pump and signal fields, respectively.  $\kappa_{\text{ex}}$  represents the dissipation associated with the input coupling of the optical cavity.

In a frame rotating at the frequency of the pump field  $a_0 = ae^{-i\omega_p t}$ , the nonlinear quantum Langevin equations of the system can be expressed as

$$\begin{aligned} \dot{a}_0 &= \left(i\Delta_0 - \frac{\kappa}{2}\right)a_0 - ig_0 a_0 (b^\dagger + b) \\ &\quad + \sqrt{\kappa_{\text{ex}}}(a_p + a_s e^{-i\Delta_s t}) + \sqrt{\kappa_0}a_v, \\ \dot{b} &= -\left(\frac{\Gamma_m}{2} + i\omega_m\right)b - ig_0 a_0^\dagger a_0 + \sqrt{\Gamma_m}b_{\text{th}}, \end{aligned} \quad (2)$$

where  $\kappa = \kappa_0 + \kappa_{\text{ex}}$  is the total decay rate of the optical cavity ( $\kappa_0$  denotes the internal loss rate of the cavity apart from  $\kappa_{\text{ex}}$ ),  $\Delta_s = \omega_s - \omega_p$  is the frequency difference between the signal and pump fields,  $\Gamma_m = \omega_m/Q_m$  is the dissipation rate of the mechanical mode,  $Q_m$  is the mechanical quality factor,  $a_v$  denotes the vacuum noise associated with the optical dissipation, and  $b_{\text{th}}$  denotes the thermal drive to the resonator.

We express the optical and mechanical modes as the sum of their mean fields at the steady state and the fluctuation term:  $a_0 = \alpha + d$ ,  $b = \beta + \delta b$ , and  $a_p = \alpha_p + d_p$ . From

Eq. (2), we can obtain the values of the mean field at the steady state for the optical cavity mode and mechanical mode as  $\alpha = \sqrt{\kappa_{\text{ex}}}\alpha_p/\frac{\kappa}{2} - i\Delta_{\text{eff}}$  and  $\beta = g_0|\alpha|^2/\omega_m$ .

By neglecting the nonlinear terms, the linearized quantum Langevin equations of  $d$  and  $\delta b$  are given by

$$\begin{aligned} \dot{d}(t) &= -\left(\frac{\kappa}{2} - i\Delta_{\text{eff}}\right)d(t) - ig_0\alpha[\delta b^\dagger(t) + \delta b(t)] \\ &\quad + \sqrt{\kappa_{\text{ex}}}a_s e^{-i\Delta_s t} + \sqrt{\kappa_{\text{ex}}}d_p + \sqrt{\kappa_0}a_v, \\ \delta\dot{b}(t) &= -\left(\frac{\Gamma_m}{2} + i\omega_m\right)\delta b(t) \\ &\quad - ig_0[\alpha^*d(t) + \alpha d^\dagger(t)] + \sqrt{\Gamma_m}b_{\text{th}}. \end{aligned} \quad (3)$$

Note that the average displacement  $\bar{x} = \beta^* + \beta$  of the mechanical resonator slightly shifts the resonance frequency of the cavity mode and results in an effective detuning of the pump laser  $\Delta_{\text{eff}} = \Delta_0 + g_0(\beta^* + \beta)$ . We neglect the small quantum fluctuations of the input pump field  $d_p$ , vacuum noise  $a_v$ , and thermal driving of mechanical motion  $\sqrt{\Gamma_m}b_{\text{th}}$  (as it is much smaller than the optical drive). Under this approximation, we convert Eq. (4) into the frequency domain using Fourier transform:

$$\begin{aligned} \chi_c^{-1}(\omega)d(\omega) &= -ig[\delta b^\dagger(\omega) + \delta b(\omega)] + \sqrt{\kappa_{\text{ex}}}a_s(\omega - \Delta_s), \\ \chi_m^{-1}(\omega)\delta b(\omega) &= -i[g^*d(\omega) + g d^\dagger(\omega)], \end{aligned} \quad (4)$$

where  $g = g_0\alpha$  is the optomechanical coupling strength and  $\chi_c^{-1}(\omega) = -i\Delta_{\text{eff}} - i\omega + \kappa/2$  and  $\chi_m^{-1}(\omega) = i\omega_m - i\omega + \Gamma_m/2$  are the optical and mechanical susceptibilities of the optical cavity and mechanical resonator, respectively. Using the relation  $[d(\omega)]^\dagger = d^\dagger(-\omega)$  and  $[\delta b(\omega)]^\dagger = \delta b^\dagger(-\omega)$ , and assuming a resonant pump laser with  $\Delta_{\text{eff}} = 0$ , we can obtain the fluctuation of the optical cavity mode arising from the optomechanical interaction:

$$\begin{aligned} d(\omega) &= d_-(\omega) + d_+(\omega), \\ d_-(\omega)|_{\Delta_{\text{eff}}=0} &= \sqrt{\kappa_{\text{ex}}}\chi_c(\omega)\alpha_s(\omega - \Delta_s) \\ &\quad \times \{1 + 2\omega_m|g|^2\chi_c(\omega)[\chi_m^*(-\omega)\chi_m(\omega)]\}, \\ d_+(\omega)|_{\Delta_{\text{eff}}=0} &= 2\sqrt{\kappa_{\text{ex}}}\chi_c^2(\omega)\alpha_s^*(\omega + \Delta_s)\omega_m|g|^2 \\ &\quad \times [\chi_m^*(-\omega)\chi_m(\omega)], \end{aligned} \quad (5)$$

where the quantum fluctuation of the signal field has been neglected. In terms of the input-output relation, the fluctuation term of the reflective field of the cavity is  $d_r(\omega) = \sqrt{\kappa_{\text{ex}}}d(\omega) - \alpha_s(\omega - \Delta_s)$ . By assuming that the dissipation induced by the input coupling of the cavity satisfies  $\kappa_{\text{ex}} = \kappa_0 = \kappa/2$ , we obtain the reflective field of the cavity as

$$\begin{aligned} d_r(\omega) &= r_-(\omega) + r_+(\omega), \\ r_-(\omega) &= \left\{ \frac{1}{\frac{\kappa}{2i\omega} - 1} + \frac{1}{\left(1 - \frac{2i\omega}{\kappa}\right)^2} \frac{4\omega_m|g|^2}{\kappa} X_m(\omega) \right\} \alpha_s(\omega - \Delta_s), \\ r_+(\omega) &= \frac{1}{\left(1 - \frac{2i\omega}{\kappa}\right)^2} \frac{4\omega_m|g|^2}{\kappa} X_m(\omega)\alpha_s^*(\omega + \Delta_s), \end{aligned} \quad (6)$$

where  $X_m^{-1} = \omega_m^2 - \omega^2 - i\omega\Gamma_m$  represents the position susceptibilities of the mechanical motion. For monochromatic signal laser input,  $\alpha_s(\omega)$  can be expressed as a delta function

$\alpha_s\delta(\omega)$ , and the fluctuation term  $d_r(\omega)$  of the reflection of the optical cavity field can be expressed as

$$d_r(\omega) = R_-(\omega)\delta(\omega - \Delta_s) + R_+(\omega)\delta(\omega + \Delta_s). \quad (7)$$

We transform the expression of Eq. (7) into the time domain:

$$d_r(t) = R_-(\Delta_s)e^{-i\Delta_s t} + R_+(-\Delta_s)e^{i\Delta_s t}. \quad (8)$$

As we considered a rotating frame at the frequency of the pump field  $\omega_p$ , in the initial frame, Eq. (8) can be rewritten as

$$d_r(t) = R_-(\Delta_s)e^{-i\omega_s t} + R_+(-\Delta_s)e^{i\omega_s t}, \quad (9)$$

where  $\omega_F = \omega_p + \Delta_s = 2\omega_p - \omega_s$  is the angular frequency of the FWM field. From Eq. (9), it is evident that the reflective field contains two components. The first term with frequency  $\omega_p$  denotes the amplified signal field, which contributes to the OMIT and OMIA phenomena, whereas the second term with frequency  $\omega_F$  denotes the generated FWM field induced by the radiation pressure coupling between the cavity field and mechanical mode. The corresponding amplitudes of the signal and FWM fields are given by

$$\begin{aligned} R_-(\Delta_s) &= \left\{ \frac{1}{\frac{\kappa}{2i\Delta_s} - 1} + \frac{1}{\left(1 - \frac{2i\Delta_s}{\kappa}\right)^2} \frac{4\omega_m|g|^2}{\kappa} X_m(\Delta_s) \right\} \alpha_s, \\ R_+(-\Delta_s) &= \frac{1}{\left(1 + \frac{2i\Delta_s}{\kappa}\right)^2} \frac{4\omega_m|g|^2}{\kappa} X_m(-\Delta_s)\alpha_s^*. \end{aligned} \quad (10)$$

Under the condition of bad cavity limit  $\kappa \gg \omega_m$ , the amplitudes of the output probe field and FWM field tend to be equal:  $R_-(\Delta_s) \approx R_+(-\Delta_s)$  around  $|\Delta_s| = \omega_m$ .

## B. Frequency response characteristics of the FWM

For better understanding of the FWM phenomenon in the unresolved sideband optomechanical system under consideration, we define the intensity magnification of the output signal and FWM fields as

$$\begin{aligned} M_-(\Delta_s) &= \frac{|R_-(\Delta_s)|^2}{|\alpha_s|^2} \\ &\approx \frac{16\omega_m^2|g|^4}{\kappa^2} |X_m(\Delta_s)|^2 + \frac{1}{1 + \kappa^2/4\Delta_s^2}, \\ M_+(-\Delta_s) &= \frac{|R_+(-\Delta_s)|^2}{|\alpha_s|^2} \approx \frac{16\omega_m^2|g|^4}{\kappa^2} |X_m(-\Delta_s)|^2. \end{aligned} \quad (11)$$

We have assumed that the system operates in the bad cavity regime  $\kappa \gg \Delta_s$ . It is evident that the frequency responses of both the output fields follow the mechanical susceptibility around the detuning frequency  $\Delta_s \approx \pm\omega_m$ .

Using Eq. (11), we investigate the frequency response characteristics of the FWM. Accordingly, a membrane-in-the-middle (MIM) system is considered herein. Notably, many prominent experiments have been reported using the MIM system, including strong cooling [20,21], generation of the optical squeezing state [22,23], conversion between microwave and optical fields [24], and OMIT and OMIA [4].

In Fig. 2, we have plotted the intensity magnification of the output signal and FWM fields as a function of the signal-pump detuning  $\Delta_s$  in units of the mechanical resonance frequency  $\omega_m$ . The parameters used are as follows:  $\kappa/2\pi = 10\text{MHz}$ ,

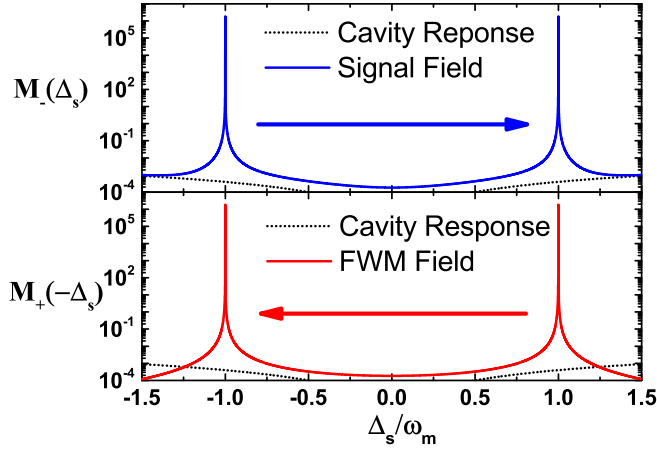


FIG. 2. Intensity magnification function of the output fields as a function of signal-pump detuning  $\Delta_s$  from  $-1.5\omega_m$  to  $1.5\omega_m$ . The amplified signal field (blue line) and FWM field (red line) have almost the same intensity around  $\Delta_s = \pm\omega_m$  and slightly different intensities at the frequency  $|\Delta_s| > \omega_m$  owing to the cavity response (black dotted line). The arrows show that the signal and FWM fields have opposite detuning vs the pump.

$\omega_m/2\pi = 100\text{kHz}$ ,  $Q_m = 10^5$ ,  $g_0/2\pi = 20\text{Hz}$ ,  $P_p = 50\ \mu\text{W}$ , and the wavelength of the laser is  $1064\ \text{nm}$ . Both the output fields present very sharp frequency responses and the corresponding bandwidth is as narrow as that of the mechanical resonator, which is in turn determined by the mechanical quality factor and mechanical resonance frequency as  $\Gamma_m = \omega_m/Q_m$ . For the MIM system considered,  $\Gamma_m = 1\text{Hz}$ , which indicates that the frequency response bandwidth of FWM is much less than the linewidth of the bare cavity.

In Fig. 3, we have plotted the intensity magnification function of the output fields as a function of the mechanical quality factor  $Q_m$  and cavity dissipation  $\kappa$ . As shown in Fig. 3(a), the intensity magnification of the output fields increases with the mechanical quality factor  $Q_m$ , but the bandwidth of intensity magnification is suppressed for higher  $Q_m$ . Furthermore, the intensity magnification depends on the optical cavity dissipation rate. Low cavity dissipation is beneficial to promote the gain of the optical fields, whereas the frequency response bandwidth of the FWM is unchanged. This is because low cavity dissipation helps to improve the intracavity photon number, which in turn increases the optomechanical coupling strength and promotes the FWM effect. However, the bandwidth of the intensity magnification function merely depends on the mechanical susceptibility [Eq. (10)] and is thus immune to the cavity dissipation.

Although only a typical mechanical quality factor  $Q_m = 10^5$  is used for simulation in Fig. 3, it is observed that the state-of-the-art mechanical quality factor ( $\text{Si}_3\text{N}_4$  membrane) has been improved to  $Q_m \sim 10^8$  and the mechanical dissipation rate has been suppressed to  $3.6\ \text{mHz}$  [25]. In this scenario, an extremely narrow response bandwidth of the FWM via the optomechanical system can be achieved in principle, which can find potential applications in the generation of an ultranarrow linewidth laser instead of a high-finesse optical cavity the linewidth of which is currently limited to  $\sim 1\ \text{kHz}$  [26,27]. Moreover, the dissipation of the mechanical resonator can be

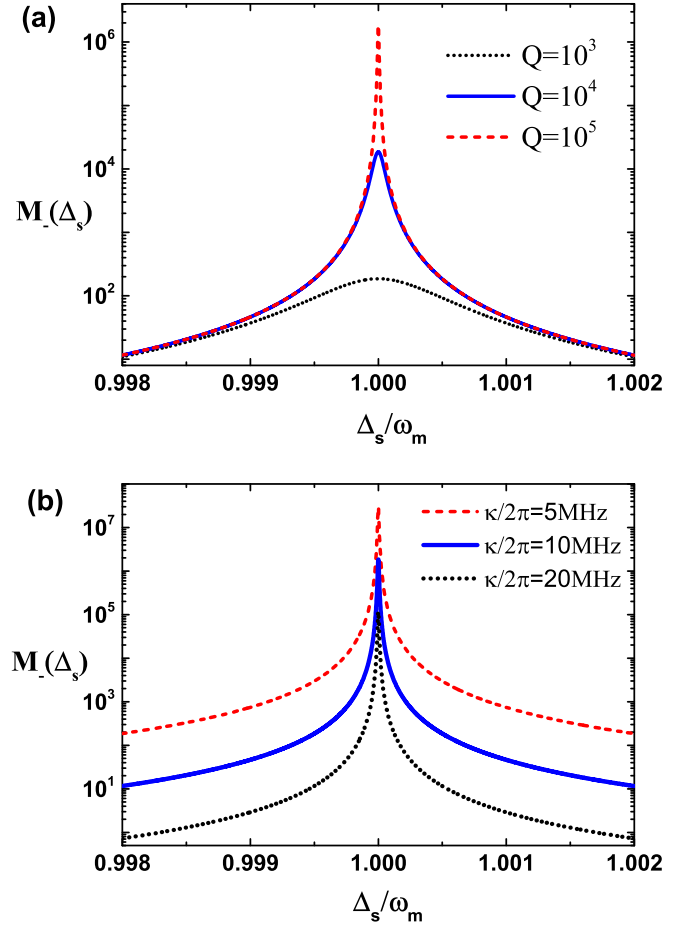


FIG. 3. Intensity magnification function of the output fields as a function of (a) mechanical quality factor  $Q_m$  and (b) cavity dissipation. The other parameters are the same as in Fig. 2.

controlled by optical damping via a feedback system [28–31] and thus a tunable bandwidth FWM process can be achieved.

### C. Maximum magnification

By setting the absolute value of the frequency difference between the signal and pump fields to be equal to the resonance frequency of the mechanical mode,  $\Delta_s = \pm\omega_m$ , the FWM process reaches its maximum magnification for both the signal and FWM fields:

$$R_{-}(\pm\omega_m) = \pm i \frac{4g_0^2 n_p}{\kappa \Gamma_m} \alpha_s = \pm i C \alpha_s,$$

$$R_{+}(\mp\omega_m) = \mp i \frac{4g_0^2 n_p}{\kappa \Gamma_m} \alpha_s^* = \mp i C \alpha_s^*,$$

$$|A|^2 \equiv M_{-}(\pm\omega_m) = M_{+}(\mp\omega_m) = C^2, \quad (12)$$

where the maximum amplitude magnification  $|A| \equiv C$ ,  $C = 4g_0^2 n_p / \kappa \Gamma_m$  represents the optomechanical cooperativity of the system, and  $n_p = |\alpha|^2$  is the mean photon number of the pump field inside the cavity. At this specific frequency detuning point, the reflected signal and FWM fields at the frequencies  $\omega_s$  and  $2\omega_p - \omega_s$  have the same strengths and opposite phases.

In order to investigate the dependence of the maximum amplitude magnification  $|A|$  on the relevant experimental

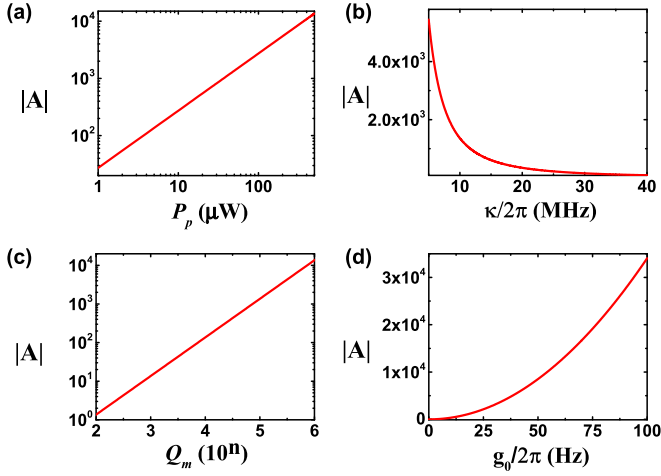


FIG. 4. Maximum amplitude magnification of the output fields as a function of (a) input pump power, (b) cavity dissipation, (c) quality factor of the mechanical resonator, and (d) single-photon optomechanical coupling strength. The other parameters are the same as in Fig. 2.

parameters, we substitute the relations  $n_p = 2n_{in}/\kappa$  and  $n_{in} = P_p/\hbar\omega_p$  into Eq. (12) and obtain the expression

$$|A| = \frac{8g_0^2 Q_m P_p}{\kappa^2 \omega_m \hbar \omega_p}. \quad (13)$$

Figure 4 shows the maximum amplitude magnification of the output fields as a function of the input pump power, cavity dissipation, quality factor of the mechanical resonator, and single-photon optomechanical coupling strength. The other parameters used are the same as in Fig. 2. It is demonstrated that the maximum amplitude magnification  $|A|$  increases in proportion to the pump power, quality factor of the mechanical resonator, and square of the coupling strength. In contrast,  $|A|$  is inversely proportional to the square of the cavity dissipation.

#### D. Added noises of the FWM

In the above, we have shown the gain characteristics of the amplified signal and FWM field without considering the added noises, which are principally induced by the thermal motion of the mechanical resonator and the quantum fluctuations of the pump field that we have neglected in Eq. (4). As the induced mechanical motion due to the quantum fluctuation of the pump field is much weaker than the thermal motion unless the mechanical resonator is around its quantum ground state [32], here we only consider the dominant noise arising from the thermal motion. We rewrite Eq. (4) by adding the thermal motion term:

$$\begin{aligned} \chi_c^{-1}(\omega)d(\omega) &= -ig[\delta b^\dagger(\omega) + \delta b(\omega)] + \sqrt{\kappa_{\text{ex}}}a_s(\omega - \Delta_s), \\ \chi_m^{-1}(\omega)\delta b(\omega) &= -i[g^*d(\omega) + gd^\dagger(\omega)] + \sqrt{\Gamma_m}b_{\text{th}}(\omega). \end{aligned} \quad (14)$$

From Eq. (14), the fluctuation of the optical cavity mode is derived:

$$\begin{aligned} d(\omega) &= d_-(\omega) + d_+(\omega) - ig\sqrt{\Gamma_m}\chi_c(\omega) \\ &\quad \times [\chi_m(\omega)b_{\text{th}}(\omega) + \chi_m^*(-\omega)b_{\text{th}}^\dagger(\omega)]. \end{aligned} \quad (15)$$

In terms of the input-output relation of the optical cavity, we obtain the reflective field of the cavity as

$$\begin{aligned} d_r(\omega) &= r_-(\omega) + r_+(\omega) - ig\sqrt{\kappa_{\text{ex}}\Gamma_m}\chi_c(\omega) \\ &\quad \times [\chi_m(\omega)b_{\text{th}}(\omega) + \chi_m^*(-\omega)b_{\text{th}}^\dagger(\omega)], \end{aligned} \quad (16)$$

where  $r_{\mp}(\omega)$  are the same as they are in Eq. (6). The third term on the right-hand side of Eq. (16) describes exactly the added noise arising from the thermal motion of the resonator. For frequency around  $\pm\omega_m$  where the gain factor of the signal field is significant, the mean thermal photon numbers per hertz at frequency  $\Delta_s$  are approximately given by

$$\begin{aligned} N_1(\Delta_s) &= \int_{\Delta_s-\pi}^{\Delta_s+\pi} \frac{d\omega}{2\pi} \kappa_{\text{ex}}\Gamma_m g^2 |\chi_c(\omega)\chi_m(\omega)|^2 \\ &\quad \times \langle b_{\text{th}}(\omega)^\dagger b_{\text{th}}(\omega) \rangle, \\ N_2(-\Delta_s) &= \int_{\Delta_s-\pi}^{\Delta_s+\pi} \frac{d\omega}{2\pi} \kappa_{\text{ex}}\Gamma_m g^2 |\chi_c(\omega)\chi_m^*(-\omega)|^2 \\ &\quad \times \langle b_{\text{th}}(\omega)b_{\text{th}}(\omega)^\dagger \rangle. \end{aligned} \quad (17)$$

For  $\Delta_s = \omega_m$ , Eq. (17) is rewritten as

$$\begin{aligned} N_1(\omega_m) &= 2Cn_{\text{th}}, \\ N_2(-\omega_m) &= 2C(n_{\text{th}} + 1), \end{aligned} \quad (18)$$

where  $n_{\text{th}} \approx k_B T_{\text{bath}}/\hbar\omega_m$  denotes the thermal phonon number of the mechanical motion. The corresponding power of the noise photons can be given by  $P_i^N(\pm\omega_m) = \hbar\omega_s N_i(\pm\omega_m)$  ( $i = 1, 2$ ). Given the same parameters as used in Fig. 2, the added noise induced by thermal motion of the resonator is 31.8 nW at room temperature  $T_{\text{bath}} = 300$  K. If the resonator is operated in a cryogenic temperature of 10 mK, the added noise can be suppressed to 1 pW.

### III. CONCLUSION AND DISCUSSION

In summary, we have investigated the FWM process in an unresolved sideband optomechanical system. The FWM process can achieve a large gain for microwatt-level pump power of the input signal field. For a zero-detuning pump, the maximum amplitude magnification of the signal and FWM fields is equal to the optomechanical cooperation  $C$ , which is determined by the dissipation of the optical cavity and mechanical modes, optomechanical coupling strength, and input pump power. We also observed that the frequency responses of both the output fields follow the mechanical susceptibility. For high- $Q$  mechanical resonators [25,33–36], the frequency response bandwidth of the signal and FWM fields can be narrowed down to the subhertz level, which can be dynamically tuned using the feedback control of mechanical motion. Moreover, our system supports multiple FWM processes simultaneously owing to the unresolved sideband regime and multimode characteristics of the mechanical resonator. When mechanical resonators with equispaced eigenfrequencies such as high-stress strings [37] are used, the multimode FWM process can produce a comblike frequency response, which may find applications in optical frequency combs [13,38,39].

The scheme presented is applicable in various optomechanical systems such as MIM [40–42], nanostrings [29,43], and photonic crystals [44,45]. Unlike atomic systems or optical nonlinear crystals, optomechanical systems can be operated in a broad wavelength range, even in the microwave band. Moreover, the low-power operation is beneficial to develop integrated optical devices. The results presented herein may have potential applications in optical atomic clocks and other related classical and quantum optical fields.

## ACKNOWLEDGMENTS

This work was supported by the Key Project of the National Key Research and Development Program of China (Grant No. 2016YFA0301403), the Natural National Science Foundation of China (Grants No. 11774209, No. 61378010, No. 11674390, and No. 91736106), the Shanxi program 1331KSC, and the Program for the Outstanding Innovative Teams of Higher Learning Institutions of Shanxi.

- 
- [1] S. Weis, R. Rivière, S. Deléglise, E. Gavartin, O. Arcizet, A. Schliesser, and T. J. Kippenberg, *Science* **330**, 1520 (2010).
- [2] A. Safavi-Naeini, T. Alegre, J. Chan, M. Eichenfield, M. Winger, Q. Lin, J. Hill, D. Chang, and O. Painter, *Nature (London)* **472**, 69 (2011).
- [3] F. Massel, T. Heikkilä, J. Pirkkalainen, S. Cho, H. Saloniemi, P. Hakonen, and M. Sillanpää, *Nature (London)* **480**, 351 (2011).
- [4] M. Karuza, C. Biancofiore, M. Bawaj, C. Molinelli, M. Galassi, R. Natali, P. Tombesi, G. Di Giuseppe, and D. Vitali, *Phys. Rev. A* **88**, 013804 (2013).
- [5] M. Maeda, P. Kumar, and J. H. Shapiro, *Opt. Lett.* **12**, 161 (1987).
- [6] M. G. Raizen, L. A. Orozco, M. Xiao, T. L. Boyd, and H. J. Kimble, *Phys. Rev. Lett.* **59**, 198 (1987).
- [7] D. M. Hope, H.-A. Bachor, P. J. Manson, D. E. McClelland, and P. T. H. Fisk, *Phys. Rev. A* **46**, R1181(R) (1992).
- [8] V. Josse, A. Dantan, L. Vernac, A. Bramati, M. Pinard, and E. Giacobino, *Phys. Rev. Lett.* **91**, 103601 (2003).
- [9] J. Ries, B. Brezger, and A. I. Lvovsky, *Phys. Rev. A* **68**, 025801 (2003).
- [10] V. Boyer, A. M. Marino, R. C. Pooser, and P. D. Lett, *Science* **321**, 544 (2008).
- [11] R. W. Boyd, *Nonlinear Optics*, 2nd ed. (Academic, San Diego, 2003).
- [12] G. P. Agrawal, *Nonlinear Fiber Optics, Fourth Edition & Application of Nonlinear Fiber Optics*, 2nd ed. (Academic, San Diego, 2003).
- [13] K. J. Karki, *Phys. Rev. A* **96**, 043802 (2017).
- [14] S. Huang and G. S. Agarwal, *Phys. Rev. A* **81**, 033830 (2010).
- [15] Z. Vernon and J. E. Sipe, *Phys. Rev. A* **92**, 033840 (2015).
- [16] W.-Z. Jia, L.-F. Wei, Y. Li, and Y.-x. Liu, *Phys. Rev. A* **91**, 043843 (2015).
- [17] X.-W. Xu and Y. Li, *Phys. Rev. A* **92**, 023855 (2015).
- [18] J. Ma, C. You, L.-G. Si, H. Xiong, J. Li, X. Yang, and Y. Wu, *Sci. Rep.* **5**, 11278 (2015).
- [19] C. Jiang, Y. S. Cui, and H. X. Liu, *Europhys. Lett.* **104**, 34004 (2013).
- [20] M. Underwood, D. Mason, D. Lee, H. Xu, L. Jiang, A. B. Shkarin, K. Børkje, S. M. Girvin, and J. G. E. Harris, *Phys. Rev. A* **92**, 061801(R) (2015).
- [21] R. W. Peterson, T. P. Purdy, N. S. Kampel, R. W. Andrews, P.-L. Yu, K. W. Lehnert, and C. A. Regal, *Phys. Rev. Lett.* **116**, 063601 (2016).
- [22] T. P. Purdy, P. L. Yu, R. W. Peterson, N. S. Kampel, and C. A. Regal, *Phys. Rev. X* **3**, 031012 (2013).
- [23] W. H. P. Nielsen, Y. Tsaturyan, C. Bo Møller, and E. S. Polzik, *Proc. Natl. Acad. Sci. U.S.A.* **114**, 62 (2017).
- [24] R. W. Andrews, R. W. Peterson, T. P. Purdy, K. Cicak, R. W. Simmonds, C. A. Regal, and K. W. Lehnert, *Nat. Phys.* **10**, 321 (2014).
- [25] Y. Tsaturyan, A. Barg, E. Polzik, and A. Schliesser, *Nature Nanotechnology* **12**, 776 (2017).
- [26] T. Kessler, C. Hagemann, C. Grebing, T. Legero, U. Sterr, F. Riehle, M. Martin, L.-S. Chen, and J. Ye, *Nat. Photonics* **6**, 687 (2012).
- [27] D. G. Matei, T. Legero, S. Hafner, C. Grebing, R. Weyrich, W. Zhang, L. Sonderhouse, J. M. Robinson, J. Ye, F. Riehle, and U. Sterr, *Phys. Rev. Lett.* **118**, 263202 (2017).
- [28] S. Mancini, D. Vitali, and P. Tombesi, *Phys. Rev. Lett.* **80**, 688 (1998).
- [29] M. Poggio, C. L. Degen, H. J. Mamin, and D. Rugar, *Phys. Rev. Lett.* **99**, 017201 (2007).
- [30] D. J. Wilson, V. Sudhir, N. Piro, R. Schilling, A. Ghadimi, and T. J. Kippenberg, *Nature (London)* **524**, 325 (2015).
- [31] A. Krause, T. Blasius, and O. Painter, [arXiv:1506.01249](https://arxiv.org/abs/1506.01249).
- [32] T. P. Purdy, R. W. Peterson, and C. A. Regal, *Science* **339**, 801 (2013).
- [33] Y. Tsaturyan, A. Barg, A. Simonsen, L. G. Villanueva, S. Schmid, A. Schliesser, and E. S. Polzik, *Opt. Express* **22**, 6810 (2014).
- [34] G. D. Cole, I. Wilson-Rae, K. Werbach, M. R. Vanner, and M. Aspelmeyer, *Nat. Commun.* **2**, 231 (2011).
- [35] Z.-Y. Li, Q. Zhang, X. You, Y.-M. Li, and K.-C. Peng, *Appl. Phys. Lett.* **109**, 191903 (2016).
- [36] R. A. Norte, J. P. Moura, and S. Groblacher, *Phys. Rev. Lett.* **116**, 147202 (2016).
- [37] A. Bokaian, *J. Sound Vib.* **142**, 481 (1990).
- [38] S. Diddams, L. Hollberg, and V. Mbele, *Nature (London)* **445**, 627 (2007).
- [39] A. Cingoz, D. Yost, T. Allison, A. Ruehl, M. Fermann, I. Hartl, and J. Ye, *Nature (London)* **482**, 68 (2012).
- [40] J. C. Sankey, C. Yang, B. M. Zwickl, A. M. Jayich, and J. G. E. Harris, *Nat. Phys.* **6**, 707 (2010).
- [41] J. Thompson, B. Zwickl, A. Jayich, F. Marquardt, S. Girvin, and J. Harris, *Nature (London)* **452**, 72 (2008).
- [42] D. J. Wilson, C. A. Regal, S. B. Papp, and H. J. Kimble, *Phys. Rev. Lett.* **103**, 207204 (2009).
- [43] V. Sudhir, R. Schilling, S. A. Fedorov, H. Schütz, D. J. Wilson, and T. J. Kippenberg, *Phys. Rev. X* **7**, 031055 (2017).
- [44] A. G. Krause, J. T. Hill, M. Ludwig, A. H. Safavi-Naeini, J. Chan, F. Marquardt, and O. Painter, *Phys. Rev. Lett.* **115**, 233601 (2015).
- [45] K. Fang, J. Luo, A. Metelmann, M. Matheny, F. Marquardt, A. Clerk, and O. Painter, *Nat. Phys.* **13**, 465 (2017).